Reflector-Based SAR Systems with Digital Beamforming: Optimizing Performance by Variable Transmit Signal Bandwidth

Sigurd Huber, Gerhard Krieger, and Alberto Moreira
German Aerospace Center (DLR), Oberpfaffenhofen, Germany

https://ieeexplore.ieee.org/document/9472701

Abstract

In recent years the complexity of space borne SAR sensors has increased dramatically. This development is mainly driven by the need of a higher mapping capability of these systems with better performance in terms of swath width, resolution and sensitivity. To deal with these challenges innovative SAR concepts have been proposed, where a significant part of the radar signal processing is carried out onboard the spacecraft. This paper identifies further optimization potentials for reflector-based SAR systems with digital beamforming. Array-fed reflectors allow the simultaneous transmission of spatially separated waveforms. This inherent property can be exploited in order to reduce the amount of data to be downlinked to ground and decrease the energy consumption of the SAR instrument at the same time.

1 Introduction

Synthetic aperture radar (SAR) imaging with spaceborne platforms has become an invaluable tool for Earth observation. As one of the most important applications, SAR data shall help establishing a better understanding of processes related to climate change. Currently, several SAR missions in different countries around the world are under development. Prominent examples are the German mission proposal Tandem-L [6, 11, 4], the European mission BIOMASS [1] or the US American / Indian mission NISAR [12]. All these missions have in common that they employ reflector-antenna-based SAR satellites. The design goal in particular for Tandem-L and NISAR is to increase their mapping capacity using very large swath widths, short revisit times and high resolution in order to serve the scientific need for high quality and quantity of data.

Swath width and resolution are design drivers in terms of power consumption of a SAR system. For instance doubling the swath width by increasing the beam width by a factor of two implies doubling the transmit power in order to have the same sensitivity. The required transmit power in turn impacts other satellite sub-systems, like the solar panels, the batteries and the heat dissipation system. By default, SAR satellites are equipped with a power source which allows transmitting a single waveform, typically a chirp signal of constant bandwidth and duration, with a certain transmit gain. From a cost point of view it could therefore prove worthy to identify optimization potentials for power saving.

Maybe an even more important consequence of ultra-wide-swath imaging with fine resolution is the enormous amount of data recorded by the SAR sensor, which has to be transferred to ground. This is in particular critical for multi-channel sensors, where several data streams are required for further processing on ground. Data volume is a clear cost driver for a SAR mission, since it determines the sizing of the data downlink system and the number of ground stations as well as data handling- and distribution-infrastructure. Usually, resolution is specified to be constant on ground over the swath as for example in the Sentinel-1 mission [13, 14]. As a consequence of the sidelooking imaging geometry this, however, implies that the pulse bandwidth would have to be continuously adapted over the swath - larger bandwidth in near range and lower bandwidth in far range. With current sate-of-the-art planar array SAR systems this is not possible. Instead, sensors like Sentinel-1 or Envisat ASAR [10] feature SAR instruments with programmable bandwidth. Wide swath imaging is performed using ScanSAR modes, where the bandwidth is adapted to a specific burst. This leads to a sawtooth-like ground range resolution profile and a certain reduction of the data volume, however, imaging wide swaths in stripmap or staggered SAR [15] mode would still not be feasible, because this would require transmitting a pulse with spatially varying bandwidth.

In order to deal with these challenges, this paper exploits the inherent properties of array-fed reflector SAR systems, where the bandwidth of the transmitted wave field is adapted to range yielding quasi constant ground range resolution. This requires a multi-channel transmitter which is capable of transmitting waveforms simultaneously with variable bandwidth and duration. The basic concept has been introduced in [7] for so called hybrid SAR modes, where a certain part of a swath is illuminated for instance with a waveform of larger bandwidth. Here, we lay the focus on a continuous adaption of the signal bandwidth and on a proper on-board processing strategy of the received SAR signal, such that the data volume can be reduced. A positive side effect of the range-adaptive waveforms is that the SAR system needs to transmit less energy without impairing the sensitivity. Finally, an optimization potential is discussed, where the transmit power is adapted to range. This would require a transmitter architecture with individ-

ual gain control in each channel. Such a design could allow reducing the SAR instrument power consumption even further.

2 Reflector SAR Principle

The main motivation to employ reflector antennas for spaceborne SAR imaging is their potential to realize very large apertures ($> 100\,\mathrm{m}^2$). The reflector is illuminated by a so-called feed array, which houses the SAR instrument, including the RF frontend with radiators as well as the digital hardware. Since each antenna beam is associated with a particular element of the feed array and has almost vanishing overlap with neighbouring beams, it is possible to radiate different waveforms in spatially separated directions, as indicated by the colored beams in Fig. 1. This concept wouldn't be compatible with planar array antennas, where the individual beams completely overlap in the far field so that an unwanted mixing of the waveforms would occur. So called defocused reflector concepts [3] might still offer enough waveform separation with some spatio-temporal waveform optimization. The concept of radiating

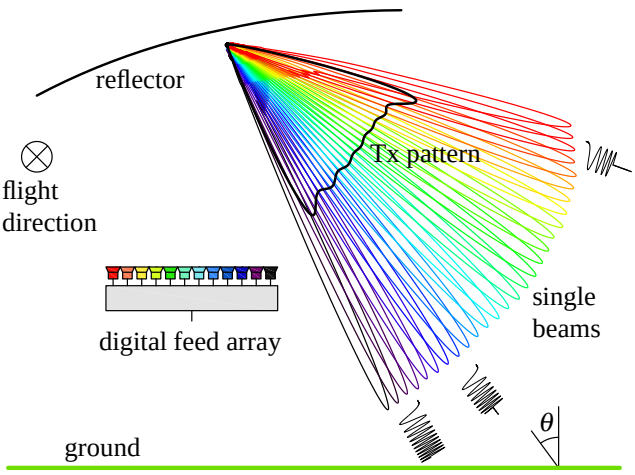

Figure 1 Side-looking reflector SAR system with digital feed array. Each feed element is associated with a quasi non-overlapping beam, indicated by the color code. This allows transmitting spatially separated waveforms.

simultaneously multiple waveforms is a MIMO principle, which found its application in new powerful SAR imaging modes [5, 8].

The broad transmit pattern, shown in Fig. 1, results from activating all feed elements simultaneously. Physically, the transmit pattern is simply the weighted[1] sum of the individual beams. On receive the beamforming strategy is different. Here, a high gain beam, dynamically steered towards the direction of the radar echo, is formed.

[1]Typically, phase-only pattern synthesis is used in oder to improve the transmit pattern.

3 Hardware Concept and Transmit Waveform Design

The functional principle of the digital feed array is shown in the block diagram of Fig. 2. Here, for a clear representation, components like filters, limiters, etc. have been omitted. The different transmit waveforms might be controlled in phase and amplitude and radiated via the feed elements. The total transmitted wave-field takes then the form

$$u_{\mathrm{Tx}}(t,\theta) = \sum_j w_j p_j(t) a_j(\theta) \ , \tag{1}$$

where w_j are complex weights for phase and amplitude control, a_j are the far field patterns of the individual beams and p_j denotes the transmit waveforms. In this context the variable θ describes the incident angle with respect to the surface normal (see Fig. 1). The azimuth dimension is not relevant for the derivation of the concept and therefore omitted.

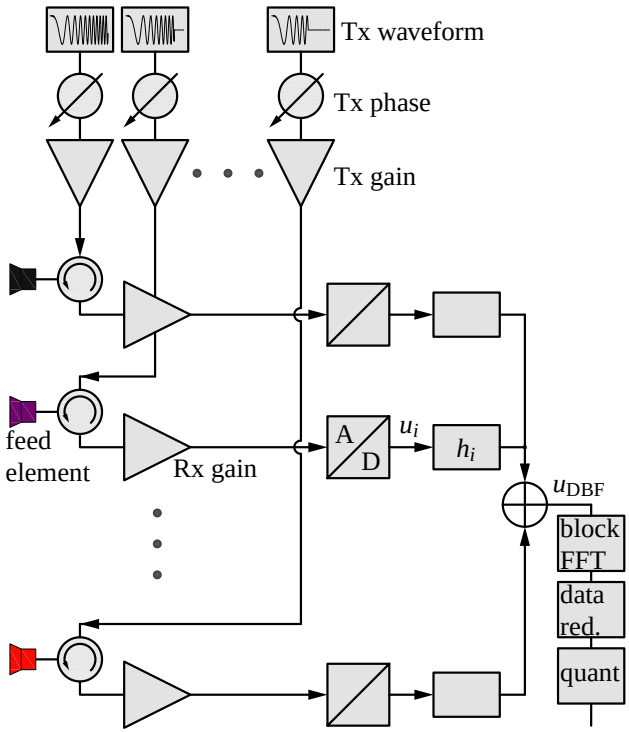

Figure 2 High level block diagram of the digital feed array and RF frontend. In each transmit (Tx) channel an individual waveform is injected. On receive, after digital beamforming using FIR filters (h_i), the signal u_{DBF} requires additional processing steps for data reduction and quantization.

On receive the radar echo signal propagates into the feed elements, the circulator and the low noise amplifiers (Rx gain) until it is digitized. At this stage the SAR signal might be written according to

$$u_i(t) \propto \int_\theta u_{\mathrm{Tx}}(t-\tau,\theta)\sigma_0(\theta)a_i(\theta)\mathrm{d}\theta \ , \tag{2}$$

with the backscatter function σ_0. Here, all constant factors as well as the range dependency (r^{-3}) have been neglected.

Assuming a monostatic imaging setup and reciprocity, the receive antenna beams are identical to the ones in the transmit case. Note, that the radar echo delay τ is a (non-linear) function of the incident angle θ.
The beamforming operation may be represented by a convolution of the received SAR signal u_i with a time-variant filter h_i followed by a summation over the digital channels (count index i)

$$u_{\mathrm{DBF}}(t) = \sum_i \sum_{t'} u_i(t-t')h_i(t,t') \tag{3}$$

Regarding the design of the transmit waveforms one might first note that for a constant ground range resolution δ_{gr} the bandwidth of the waveform obeys the following relation

$$B(\theta) = \alpha \cdot \frac{c}{2\delta_{gr}\sin\theta}\ , \tag{4}$$

where α is a factor accounting for range spectrum weighting ($\alpha = 0.89$ for a rectangular window). In the simplest case one could adopt a classical chirp waveform

$$p_j(t) = \mathrm{rect}(t;\tau_{\mathrm{p},j})\mathrm{e}^{\mathrm{j}\pi(B_j/\tau_{\mathrm{p},j})t^2}\mathrm{e}^{\mathrm{j}2\pi f_c t} \tag{5}$$

of bandwidth B, duration τ_{p} and carrier frequency f_{c}. One possibility to choose a discrete set of bandwidths B_j is to select the bandwidth at the direction of maximum gain of an individual feed element. The choice of the pulse lengths $\tau_{\mathrm{p},j}$ underlies another constraint imposed by the beamforming operation (3), which requires a constant chirp rate κ,

$$\kappa = \frac{B_j}{\tau_{\mathrm{p},j}} = \text{constant}\ . \tag{6}$$

With such a waveform design the signal bandwidth and duration changes only gradually from channel to channel. To illustrate this, consider the normalized raw data signal u_{DBF} plotted in Fig. 3. Here, ideal beamforming has been assumed (no processing artefacts) and the backscatter function has been set to one. 15 targets have been evenly spaced

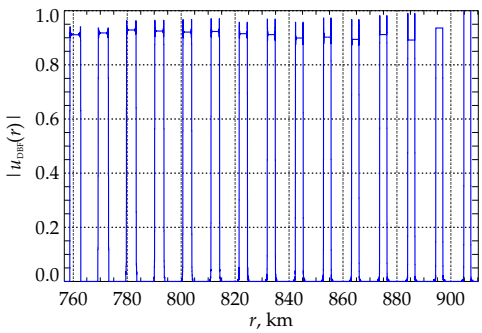

Figure 3 Example of a raw data signal, where 15 discrete scatterers have been simulated. The waveforms have been designed such that the pulse bandwidth and duration gradually decreases towards far range.

in slant range r, respective delay time τ. One might notice that the waveforms become shorter towards far range, but no significant deviations from the rectangular waveform envelope can be observed. Note, the variation of the magnitude of the individual echoes stem from the transmit patterns a_j in equation (1), where the transmit weights w_j have been set to one.

4 Data Reduction Concept

Referring to Fig. 2, after the summation node the signal $u_{\mathrm{DBF}}(t)$ is sampled with a constant rate, proportional to the signal bandwidth B at near range and some over-sampling. This is because here, due to the nonlinear relation between incident angle and bandwidth (see equation (4)), the largest bandwidth occurs. The idea of the data reduction concept is based on a time-frequency domain expansion of the signal after beamforming. Applying a short-time Fourier transform (STFT) on our example signal of Fig. 3 yields a 2-D data field as shown in Fig. 4. Here, the adaption

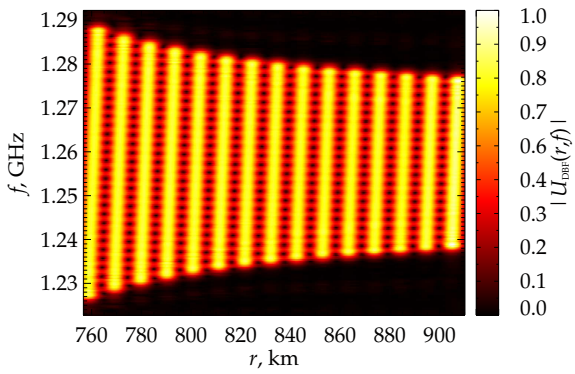

Figure 4 Short-time Fourier transform of the example signal shown in Fig. 3. This representation reveals the range dependency of the chirp waveforms with constant chirp rate.

of the pulse bandwidth to range becomes evident. Since a constant chirp rate has been employed, also the pulse duration shrinks in proportion. In this example the waveform is spectrally centered around the carrier frequency of 1.2575 GHz with a maximum bandwidth of 63.1 MHz corresponding to a ground range resolution of 5 m for the assumed imaging geometry. In this time-frequency representation the black areas would contain thermal noise which will be filtered out and by this the amount of SAR data can be reduced. In practice however, the STFT might have to be replaced by something simpler. For instance one could apply a Fast Fourier transform (FFT) on blocks of the data stream. In the example shown in Fig. 5 a block size of 128 samples has been used.
After the data reduction step, where the spectral parts containing noise have been removed, the data must be quantized. Here, traditional approaches like block adaptive quantization are of interest. But also more sophisticated concepts, where for instance samples of the block spectra are quantized according to their signal-to-noise ratio (SNR) (see for example [9]), could be considered. Spectral parts with lower SNR would require less quantization bits.

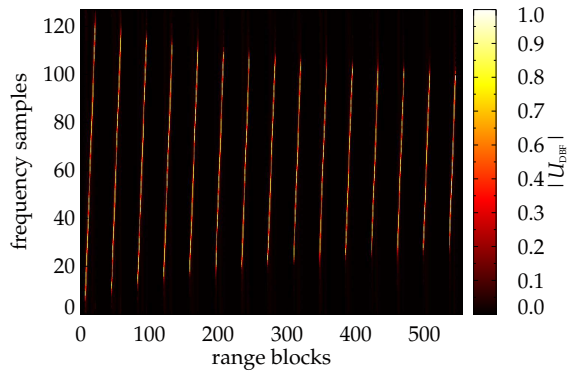

Figure 5 Block-wise Fast Fourier transform of the example signal shown in Fig. 3. Here, consecutive blocks of 128 input samples have been processed.

These three steps, blockwise FFT, data reduction by means of spectral filtering and quantization conclude the onboard data processing and the data are stored in the mass memory before they are downlinked to a ground station.

In the following the data saving potential shall be estimated. Conventionally, with constant bandwidth waveforms the data rate R is proportional to the maximum bandwidth $B_{\max}$

$$R \propto B_{\max} \ , \tag{7}$$

dictated by the ground range resolution in near range. With the proposed data reduction scheme the new rate R' becomes proportional to the average of the bandwidth as a function of the incident angle

$$R' \propto \frac{1}{\Delta\theta} \int B(\theta) \mathrm{d}\theta \ . \tag{8}$$

Substituting equation (4), this integral has the analytic solution

$$R' \propto \alpha \cdot \frac{c}{2\delta_{gr}} \frac{1}{\Delta\theta} \ln |\arctan(\theta/2)| \Big|_{\theta_{\min}}^{\theta_{\max}} \ . \tag{9}$$

The saving of data volume can now be evaluated as function of the swath width as presented in Fig. 6. Here, as additional parameter, different orbital heights have been considered. The minimum incident angle $\theta_{\min}$ is taken at 25°. As example, for Tandem-L (orbit height 750 km, swath width 350 km) the saving would be 25.1 %. Lower orbits seem to profit from higher data rate savings. The same is true for smaller minimum incident angles. Due to the proportionality of pulse bandwidth and duration the power saving follows exactly the same curves as in Fig. 6.

5 Discussion and Conclusion

The data reduction concept presented in this paper is motivated by the fact that requirements on ground range resolution are typically served by transmitting waveforms with constant bandwidth. Since the ground range resolution requires more bandwidth in near range compared to far

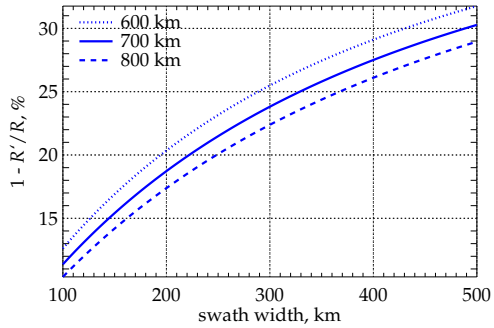

Figure 6 Saving of data rate versus swath width and for different orbit heights.

range, there is a significant data saving potential. At the same time these range adaptive waveforms allow saving transmit energy.

Synthetic aperture radar imaging at low frequencies, say in L- or P-band, becomes increasingly sensitive to ionospheric effects. A common approach to estimate and correct ionospheric phase is by means of the so called split spectrum technique (see for example [2] and references therein). The method requires transmitting and receiving an additional pulse, which is spectrally separated from the signal pulse as far as possible. Looking at Fig. 4 one could think of placing the signal spectrum at the lower (or higher) edge of the entire spectrum and the calibration pulse at the opposite end. Filtering out the noise-only parts could still offer a formidable data saving potential.

Another interesting opportunity to save even more energy arises from the fact that the SNR in a SAR image varies with range according to

$$SNR \propto \frac{\sigma_0}{r^3 \sin\theta} \ . \tag{10}$$

This typically means that the sensitivity requirement is overfulfilled in near range, while system designers struggle to direct sufficient power to the far end of the swath. A system with individual Tx gain control in each channel, as sketched in the block diagram of Fig. 2 could easily compensate at least for the distance term and the incident angle dependency.

The potential of saving data volume as well as energy consumption of the SAR instrument has to be traded off against additional hardware complexity. The application of conventional transmit/receive modules seems questionable for ultra-wide-swath imaging systems. Instead a clear separation in a transmit block and a receive block offers advantages. Moreover, the reduced data volume to be downlinked to the ground stations could allow for significant cost savings in the data handling and distribution infrastructure. Insofar, the disadvantage of a more complex transmitter and data reduction hardware could be outweighed by the presented data reduction concept.

6 Literature

[1] M. Arcioni, P. Bensi, M. Fehringer, F. Fois, F. Heliere, C.-C. Lin, and K. Scipal, "The Biomass Mission, Status of the Satellite System," in *IEEE International Geoscience and Remote Sensing Symposium (IGARSS)*, Jul 2014, pp. 1413–1416.

[2] G. Gomba, A. Parizzi, F. D. Zan, M. Eineder, and R. Bamler, "Toward Operational Compensation of Ionospheric Effects in SAR Interferograms: The Split-Spectrum Method," *IEEE Transactions on Geoscience and Remote Sensing*, vol. 54, no. 3, pp. 1446–1461, Mar 2016.

[3] S. Huber, M. Younis, G. Krieger, and A. Moreira, "A Dual-Focus Reflector Antenna for Spaceborne SAR Systems with Digital Beamforming," *IEEE Transactions on Antennas and Propagation*, vol. 61, no. 3, pp. 1461–1465, Mar 2013.

[4] S. Huber, F. Q. de Almeida, M. Villano, M. Younis, G. Krieger, and A. Moreira, "Tandem-L: A Technical Perspective on Future Spaceborne SAR Sensors for Earth Observation," *IEEE Transactions on Geoscience and Remote Sensing*, vol. 56, no. 8, pp. 4792–4807, Aug 2018.

[5] G. Krieger, N. Gebert, and A. Moreira, "Multidimensional Waveform Encoding for Synthetic Aperture Radar Remote Sensing," in *IET International Conference on Radar Systems*, Oct 2007.

[6] G. Krieger, I. Hajnsek, K. Papathanassiou, M. Eineder, M. Younis, F. D. Zan, P. Prats, S. Huber, M. Werner, H. Fiedler, A. Freeman, P. Rosen, S. Hensley, W. Johnson, L. Veilleux, B. Grafmüller, R. Werninghaus, R. Bamler, and A. Moreira, "The Tandem-L Mission Proposal: Monitoring Earth's Dynamics with High Resolution SAR Interferometry," in *IEEE Radar Conference*, May 2009.

[7] G. Krieger, I. Hajnsek, K. P. Papathanassiou, M. Younis, and A. Moreira, "Interferometric Synthetic Aperture Radar (SAR) Missions Employing Formation Flying," *Proceedings of the IEEE*, vol. 98, no. 5, pp. 816–843, May 2010.

[8] G. Krieger, M. Younis, S. Huber, F. Bordoni, A. Patyuchenko, J. Kim, P. Laskowski, M. Villano, T. Rommel, P. Lopez-Dekker, and A. Moreira, "Digital Beamforming and MIMO SAR: Review and New Concepts," in *European Conference on Synthetic Aperture Radar (EUSAR)*, Apr 2012, pp. 11–14.

[9] M. Martone, M. Villano, M. Younis, and G. Krieger, "An Efficient Onboard Quantization Strategy for Multi-Channel SAR Systems," in *12th European Conference on Synthetic Aperture Radar (EUSAR)*, Jun 2018.

[10] P. J. Meadows and P. A. Wright, "ASAR Image Mode Product Quality," in *IEEE International Geoscience and Remote Sensing Symposium (IGARSS)*, vol. 2, Jul 2003.

[11] A. Moreira, G. Krieger, I. Hajnsek, K. Papathanassiou, M. Younis, P. Lopez-Dekker, S. Huber, M. Villano, M. Pardini, M. Eineder, F. D. Zan, and A. Parizzi, "Tandem-L: A Highly Innovative Bistatic SAR Mission for Global Observation of Dynamic Processes on the Earth's Surface," *IEEE Geoscience and Remote Sensing Magazine*, vol. 3, no. 2, pp. 8–23, Jun 2015.

[12] P. Rosen, Y. Kim, H. Eisen, S. Shaffer, L. Veilleux, S. Hensley, M. Chakraborty, T. Misra, R. Satish, D. Putrevu, and R. Bhan, "A dual-frequency Spaceborne SAR Mission Concept," in *IEEE International Geoscience and Remote Sensing Symposium (IGARSS)*, Jul 2013, pp. 2293–2296.

[13] F. Rostan, S. Riegger, W. Pitz, R. Croci, and R. Torres, "The C-SAR Instrument Design & Performance for the GMES Sentinel-1 Mission," in *7th European Conference on Synthetic Aperture Radar (EUSAR)*, Jun 2008.

[14] P. Snoeij, E. Attema, M. Davidson, B. Duesmann, N. Floury, G. Levrini, B. Rommen, and B. Rosich, "The Sentinel-1 Radar Mission: Status and Performance," in *International Radar Conference (RADAR)*, Oct 2009.

[15] M. Villano, G. Krieger, and A. Moreira, "Staggered SAR: High-Resolution Wide-Swath Imaging by Continuous PRI Variation," *IEEE Transactions on Geoscience and Remote Sensing*, vol. 52, no. 7, pp. 4462–4479, Jul 2014.